Available online at www.sciencedirect.com
ScienceDirect
Bioorganic & Medicinal Chemistry Letters 17 (2007) 2293–2298
Bioorganic & Medicinal Chemistry Letters

Structure-based design of benzylamino-acridine compounds as G-quadruplex DNA telomere targeting agents

Cristina Martins,[a] Mekala Gunaratnam,[a] John Stuart,[a] Vaidahi Makwana,[a] Olga Greciano,[a] Anthony P. Reszka,[a] Lloyd R. Kelland[b] and Stephen Neidle[a,*]

[a]*CRUK Biomolecular Structure Group, The School of Pharmacy, University of London, 29-39 Brunswick Square, London WC1N 1AX, United Kingdom*

[b]*Antisoma Laboratories, St. George's Hospital Medical School, Cranmer Terrace, London SW17 0QS, United Kingdom*

Received 4 December 2006; revised 16 January 2007; accepted 18 January 2007
Available online 25 January 2007

Abstract—The design, synthesis, biophysical and biochemical evaluation is presented of a new series of benzylamino-substituted acridines as G-quadruplex binding telomerase inhibitors. Replacement of the previously reported anilino substituents by benzylamino groups results in enhanced quadruplex interaction, and for one compound, superior telomerase inhibitory activity.

Telomeres are specialized nucleoprotein structures at the ends of eukaryotic chromosomes protecting them from degradation and recombination, and allow the DNA damage response to distinguish between double-strand breaks and natural chromosome ends.[1,2] Telomeric DNA comprises tandem repeats of simple G-rich DNA sequence motifs (TTAGGG in human telomeres), typically several kilobases in length. The extreme 3′ terminus of telomeric DNA (ca. 150–200 nucleotides) is single-stranded. This single-stranded overhang is associated with the hPOT1 protein,[3] which plays a key role in the regulation of telomere length. Telomeres progressively shorten in somatic cells at successive rounds of replication. As a consequence of the 'end-replication' effect, DNA polymerase is unable to fully replicate the blunt ends. When telomeres reach a critically short length, cells enter a replicative senescence state and division no longer occurs.[4]

All human cancer cells maintain the integrity of telomere length.[5] Over 80% do so by up-regulation of the reverse transcriptase enzyme telomerase, which catalyses the synthesis of telomeric DNA repeats,[6] thereby stabilising telomeres and contributing to cellular immortalisation and oncogenesis.[7] The telomerase enzyme complex comprises two principal components, a catalytic domain (hTERT) and an RNA template (hTR), and various approaches have been devised to target one or other as an anticancer strategy.[8] A modified oligonucleotide targeting hTR has recently entered Phase I clinical trial.[9] Another approach targets the substrate, the 3′ single-stranded end of telomeric DNA, and uses small molecules to induce its folding into quadruplex structures, which are inaccessible to the RNA template component of the telomerase complex.[10] A large number of such small molecules have been reported,[11] which bind quadruplex DNA and efficiently inhibit telomerase. Most of them are based on a polycyclic aromatic core that interacts by π–π stacking with the planar G-tetrad motif of a quadruplex,[12] and have cationic side chains that interact with the negatively charged phosphate backbones in G-quadruplexes.

We have previously reported[13] on a number of 3,6,9-trisubstituted acridine molecules, one of which, BRACO-19 (compound **1**: Table 1), has been studied in detail. It produces cell growth arrest, chromosomal end-to-end fusions,[14] and anticancer activity in tumour xenografts,[15] all within a short time after exposure, contrary to the paradigm that extended exposure to telomerase inhibitors is necessary in order to induce anticancer effects. It also, in common with the natural product telomestatin,[16] competes with hPOT1 for binding to the single-strand telomeric DNA overhang, thereby inducing it to fold into a quadruplex structure.[17] The

Keywords: G-quadruplex; Acridines; Telomerase.
* Corresponding author. Tel.: +44 207 753 5969; fax: +44 207 753 5970; e-mail: stephen.neidle@pharmacy.ac.uk

0960-894X/$ - see front matter © 2007 Published by Elsevier Ltd.
doi:10.1016/j.bmcl.2007.01.056

Table 1. Data for FRET-based ΔT_m values (°), telomerase inhibition (μM) and cell growth inhibition (μM) for the trisubstituted acridines

Compound	Benzylamine	R1	FRET (ΔT_m)	TRAP EC_{50}	DU145	MCF7	A549
1	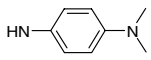	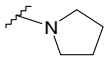	28	0.12	2.3	2.53	2.42
2	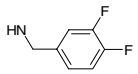	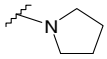	29.5	0.03	9.75	2.26	2.11
3	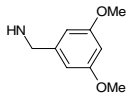	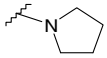	32.5	0.35	10.44	3.72	4.57
4	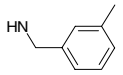	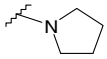	29.5	1	10	3	1.19
5	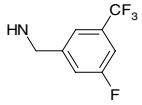	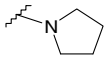	30.5	0.24	2.53	1	2
6	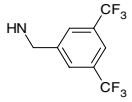	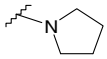	27.5	0.86	2.61	1.07	6.3
7	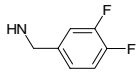	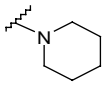	26.5	0.88	2.25	0.52	1.2
8	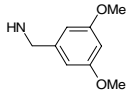	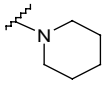	30	0.44	0.47	0.2	0.37
9	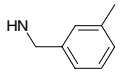	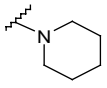	31	0.23	0.77	0.46	0.5
10	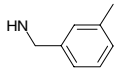	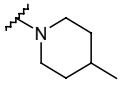	24	0.39	0.63	0.58	0.57
11	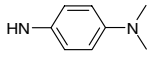	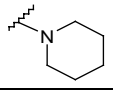	21	0.36	2.57	0.54	2

identification of BRACO-19 as a potent G-quadruplex binding molecule and telomerase inhibitor has led to the concept of these molecules as Telomere Targeting Agents, whose selective action is due to the uncapping of telomerase from telomere ends, resulting in the induction of a rapid DNA damage response and selective cell death.

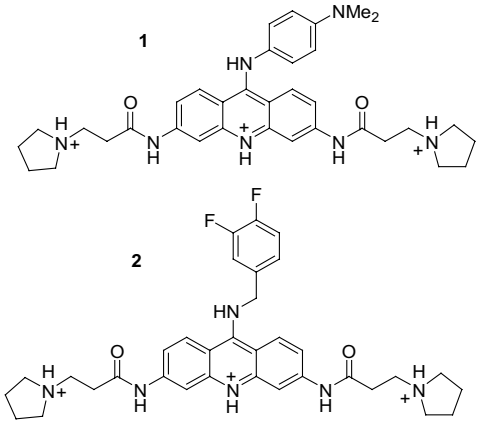

This report describes an approach to maximizing quadruplex target affinity and biological activity for 3,6,9-trisubstituted acridines by rationally altering a key structural feature in these molecules, the 9-substituent, which in BRACO-19 and analogues is an aniline group. We have used as a starting-point for structure-based design the crystal structure of the potassium form of the intramolecular 22-mer human quadruplex,[18] which has an all-parallel topology for the backbone.[19] This structure, with its propeller loops and large G-tetrad surface area (the G-platform), has been used to represent the quadruplex fold formed from the single-stranded telomeric DNA overhang in the crowded environment of the cell nucleus, in accord with observations that the all-parallel form predominates in polyethylene glycol solution.[20] We cannot exclude the possibility of other topologies for the human intramolecular quadruplex, such as the mixed parallel–antiparallel arrangement reported in NMR studies,[21] although the sequences analysed in these studies have been modified from wild-type telomeric repeats.

A simulated-annealing and molecular dynamics protocol[22] was used to explore possible ligand binding modes and located a plausible low-energy binding geometry for compound **1** (BRACO-19) with the quadruplex structure. This geometry for an acridine-quadruplex complex is distinct from that reported previously[13] using the antiparallel NMR-derived quadruplex structure[23] and has a 6.6 kcal mol^{-1} lower free energy of binding. In this new arrangement the central acridine core stacks on two guanines of the G-platform and both the 3- and 6-side chains straddle the second loop of the quadruplex. The cationic pyrrolidino end-groups are held in the binding pockets formed by the TTA loops of the quadruplex. The 9-substituent *N*-dimethylanilino group is non-coplanar with the acridine ring due to steric hindrance and is orientated out of the plane of the G-platform (Fig. 1). We envisaged that adding an additional methylene linker at the 9-position would enable the benzyl ring to be more coplanar with the G-platform (Fig. 1), thereby improving its affinity to human telomeric quadruplex DNA. The effects of substituents on the benzyl ring such as fluorine or methoxy on quadruplex affinity were explored, to ascertain if they would help to counter the steric effects of the non-planar methylene bridge. It was also reasoned that judicious choice of substituents would enhance the lipophilicity and hence uptake of these polar compounds and improve their pharmacokinetic features. Fluorine substitution would also improve stability against oxidative metabolism. Molecular dynamics simulations of the G-quadruplex complexes for **1** and **2** were undertaken using the AMBER package[24] and binding energies calculated using the Poisson-Boltzmann continuum solvent model. This gave the relative binding free energies of **1** and **2** as -25.7 ± 0.2 and -28.4 ± 0.2 kcal mol^{-1}, respectively.

In order to test the benzylamine hypothesis and generate some further compounds for subsequent pharmacological evaluation, a small focussed library of ten 3,6,9-benzylamino derivatives has been synthesised as described in Scheme 1.[26] Only the most conservative of changes were made to the 3,6-side chains, in accord with previous structure–activity studies,[13] which have found that the pyrrolidino- and piperidino-propionamido substituents are of optimal size and chain length.

Variation of substituents on the benzyl ring was restricted to simple electron-donating and withdrawing groups. A detailed synthetic route to these 3,6,9-trisubstituted acridines has been described previously[13] with the exception of the final step, which has been modified for the present compounds, enabling the final product to be precipitated out in the salt form (Scheme 1). All final compounds were isolated as the free bases from a solvent mixture of DCM/dilute ammonia and were subsequently used as such for biophysical and biological studies.

All compounds were evaluated for their ability to bind and stabilise G-quadruplex structures by a modified fluorescence resonance energy transfer (FRET) assay[27,28] using the 21-mer d[GGG(TTAGGG)$_3$] oligonucleotide end-labelled with a fluorescent donor–acceptor pair, and the change in donor/acceptor excitation emission monitored with respect to temperature. The resulting ΔT_m values provide an indication of the stability of a given ligand-quadruplex complex. Human telomerase enzyme inhibition was measured in a modified telomerase repeat amplification protocol (TRAP) assay,[29] and results are expressed as $^{tel}EC_{50}$ values. Compounds were also evaluated for in vitro cell growth inhibition, expressed as IC_{50} values, using the sulforhodamine B (SRB) assay in three human tumour cell lines, DU145 (prostate), MCF7 (breast carcinoma) and A549 (non-small cell lung carcinoma). Results are presented in Table 1, which also shows the structures of individual members of the series.

In general all of the compounds are effective G-quadruplex stabilisers. They produced changes in ΔT_m in the range of 21.0–32.5° at a ligand concentration of 1 μM. Data at other ligand concentrations (available as Supplementary Data) show the same overall trends. The majority of compounds produced an increase in ΔT_m values when compared to compound **1** (BRACO-19), with **3** showing the greatest ability to stabilise human G-quadruplex DNA, with a difference in ΔT_m of 4.5° at 1 μM compared to **1**. This broadly supports the hypothesis that the effects of the benzyl group at the 9-position result in enhanced quadruplex affinity. Compounds **3** and **8**, with –OMe substituents,

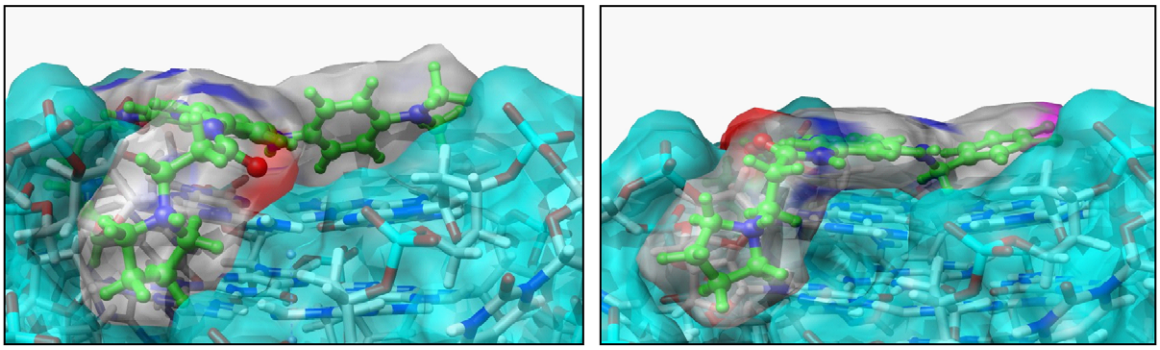

Figure 1. Solvent-accessible surface representations[25] of the low-energy quadruplex-ligand complexes from simulated annealing/molecular dynamics simulations. Carbon atoms of the ligand are coloured green. The complex with compound **1** is on the left, with the *N*-dimethylanilino ring orientated ca. 45° to the G-platform. The complex with compound **2** is on the right, with the benzyl ring stacked approximately parallel to the G-platform.

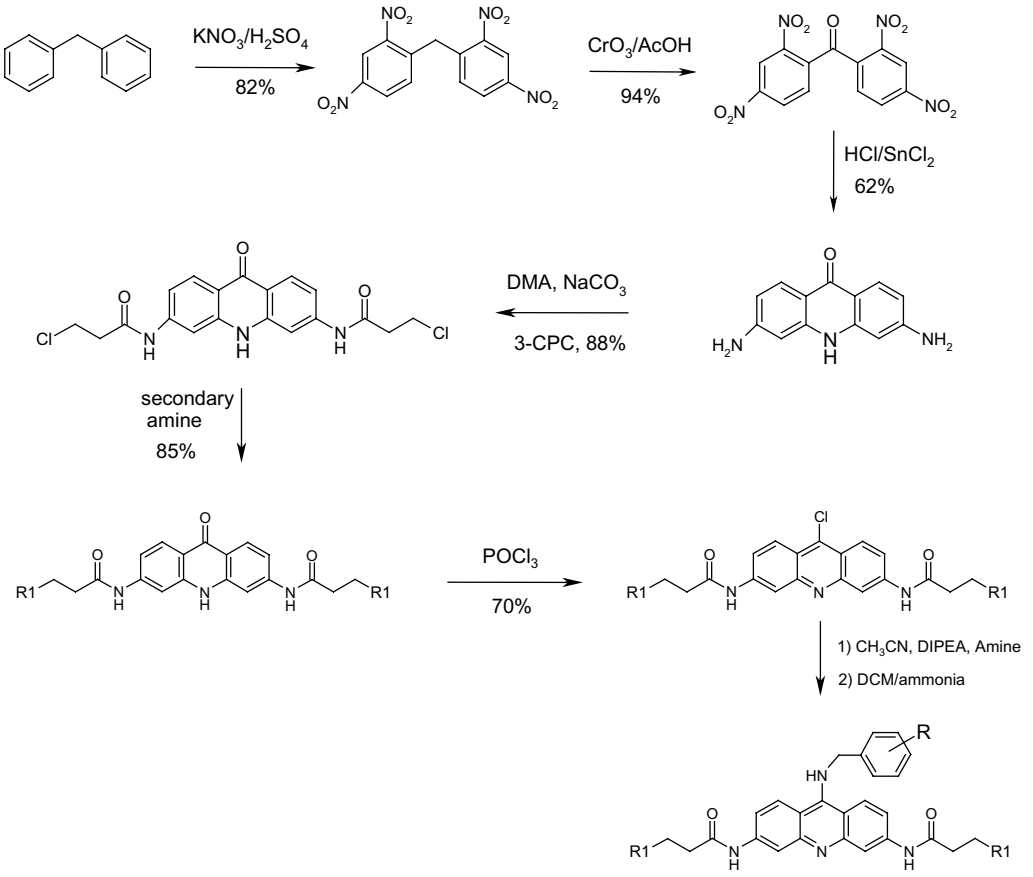

Scheme 1. Synthetic route to the benzylamino-substituted acridines. In the final step, 8.0 g (16.2 mmol) of the 9-chloro was suspended in 250 mL acetonitrile. 2.6 g (17.8 mmol) DFBA and 2.3 g (17.8 mmol) DIPEA were added and the mixture heated to reflux for 28 h. The solid was collected by filtration of the hot reaction mixture and washed twice with hot acetonitrile and dried under vacuum. The product was obtained as a yellow solid in (8.32 g) 87%.

are more effective than **2** and **7**, with strongly electron-withdrawing –F substituents, suggesting that the effects are both steric and electronic. The greater bulk when two $-CF_3$ groups are present, in compound **6** in particular, has a deleterious effect on binding (shown by, for example, compound **5 > 2 > 6**), as does the replacement of the pyrrolidino rings at the 3,6-positions with piperidino ones. An exception to this is the superior stabilising ability of **9** compared to **6**; the reasons for this are not apparent. Even so, compounds **7** and **8** are significantly superior quadruplex binders than the piperidino analogue of BRACO-19, compound **11**. Molecular modelling suggests that the piperidino are slightly too large for optimal fitting into the quadruplex grooves (Fig. 1); compound **10**, which also has an extra methyl substituent on this ring, is unsurprisingly a weaker binder and is the least potent compound in this group. Compounds **4** and **9** are as potent quadruplex binders as **2** indicating that the presence of the methyl group on the benzyl ring can be tolerated, in accord with the structural model. Table 1 shows that benzylamino substituents in the 9-position bearing electron-withdrawing groups (such as **2** and **5**) have lower ΔT_m values than the analogues bearing electron-donating groups. This is to be expected since the benzyl ring lies close to the cationic channel of the quadruplex, which would thus contribute to its binding.

All of the compounds in this series inhibit telomerase with $^{tel}EC_{50}$ values <1 μM. There is no simple correlation between $^{tel}EC_{50}$ and ΔT_m values, or with short-term cell kill (IC_{50} values). As previously observed[13] effective quadruplex stabilisation is a necessary element but by itself is not sufficient for telomerase inhibitory potency. It also has to be borne in mind that ΔT_m values are not equivalent to association constants, and so high correlations with biochemical and biological measures of activity should not be expected. Even so, it is apparent that high ΔT_m values are consistently associated with telomerase potency as estimated by $^{tel}EC_{50}$ values. The most potent telomerase inhibitor, compound **2**, has given an increased ΔT_m value compared to **1**, of 1.5°, but this is significantly less than that for **3**. The increased short-term cell kill potency observed for the piperidino compounds **7**–**10** compared to their pyrrolidino counterparts **2**–**4** appears to be due to the increased lipophilicity of the former group, and is not related to telomerase inhibition. The calculated log *P* values for **2** and **7**, for example, are 1.59 and 2.35, and are a consequence of the additional two carbon atoms at the ends of the side chains.

The favourable ΔT_m and $^{tel}EC_{50}$ values for compound **2** compared to **1** (BRACO-19), together with its improved lipophilicity and pharmacokinetic behaviour (to be published), have led to the selection of **2** as a potential clinical candidate molecule. In vivo antitumour data for **2** will be reported elsewhere, but off-target toxicity has been more recently observed, and further compounds with diminished toxicity are now being evaluated.

Acknowledgments

We are grateful to Cancer Research UK and Antisoma Ltd for support of these studies.

Supplementary data

Supplementary data associated with this article can be found, in the online version, at doi:10.1016/j.bmcl.2007.01.056.

References and notes

1. McEachern, M. J.; Krauskopf, A.; Blackburn, E. H. *Annu. Rev. Genet.* **2000**, *34*, 331.
2. Bryan, T. M.; Cech, T. R. *Curr. Opin. Cell. Biol.* **1999**, *11*, 318.
3. Zaug, A. J.; Podell, E. R.; Cech, T. R. *Proc. Natl. Acad. Sci. U.S.A.* **2005**, *102*, 10864.
4. Huq, N.; Ligner, J. *Chromosoma* **2006**, *115*, 413.
5. Autexier, C.; Lue, N. F. *Annu. Rev. Biochem.* **2006**, *75*, 493.
6. (a) Kim, N. W.; Piatyszek, M. A.; Prowse, K. R.; Harley, C. B.; West, M. D.; Ho, P. L. C.; Coviello, G. M.; Wright, W. E.; Weinrich, R.; Shay, J. W. *Science* **1994**, *266*, 2011; (b) Counter, C. M.; Hirte, H. W.; Bacchetti, S.; Harley, C. M. *Proc. Natl. Acad. Sci. U.S.A.* **1994**, *91*, 2900; (c) Shay, J. W.; Bacchetti, S. *Eur. J. Cancer* **1997**, *33*, 787.
7. Boehm, J. S.; Hession, M. T.; Bulmer, S. E.; Hahn, W. C. *Mol. Cell. Biol.* **2005**, *25*, 6464.
8. Shay, J. W.; Wright, W. E. *Nat. Rev. Drug Disc.* **2006**, *5*, 577.
9. Dikmen, Z. G.; Gellert, G. C.; Jackson, S.; Gryaznov, S.; Tressler, R.; Dogan, P.; Wright, W. E.; Shay, J. W. *Cancer Res.* **2005**, *65*, 7866.
10. Sun, D.; Thompson, B.; Cathers, B. E.; Salazar, M.; Kerwin, S. M.; Trent, J. O.; Jenkins, T. C.; Neidle, S.; Hurley, L. H. *J. Med. Chem.* **1997**, *40*, 2113.
11. For recent examples of potent ligands, see (a) Kim, M. Y.; Vankayalapati, H.; Shin-Ya, K.; Wierzba, K.; Hurley, L. H. *J. Am. Chem. Soc.* **2002**, *124*, 2098; (b) Leonetti, C.; Amodei, S.; D'Angelo, C.; Rizzo, A.; Benassi, B.; Antonelli, A.; Elli, R.; Stevens, M. F. G.; D'Incalci, M.; Zupi, G.; Biroccio, A. *Mol. Pharmacol.* **2004**, *66*, 1138; (c) Pennarun, G.; Granotier, C.; Gauthier, L. R.; Gomez, D.; Hoffschir, F.; Mandine, E.; Riou, J.-F.; Mergny, J.-L.; Maillet, P.; Boussin, F. D. *Oncogene* **2005**, *24*, 2917.
12. Haider, S. M.; Parkinson, G. N.; Neidle, S. *J. Mol. Biol.* **2003**, *326*, 117.
13. (a) Read, M.; Harrison, R. J.; Romagnoli, B.; Tanious, F. A.; Gowan, S. H.; Reszka, A. P.; Wilson, W. D.; Kelland, L. R.; Neidle, S. *Proc. Natl. Acad. Sci. U.S.A.* **2001**, *98*, 4844; (b) Harrison, R. J.; Cuesta, J.; Chessari, G.; Read, M. A.; Basra, S. K.; Reszka, A. P.; Morrell, J.; Gowan, S. M.; Incles, C. M.; Tanious, F. A.; Wilson, W. D.; Kelland, L. R.; Neidle, S. *J. Med. Chem.* **2003**, *46*, 4463; (c) Moore, M. J.; Schultes, C. M.; Cuesta, J.; Cuenca, F.; Gunaratnam, M.; Tanious, F. A.; Wilson, W. D.; Neidle, S. *J. Med. Chem* **2006**, *49*, 582.
14. Incles, C. M.; Schultes, C. M.; Kempski, H.; Koehler, H.; Kelland, L. R.; Neidle, S. *Mol. Cancer Ther.* **2004**, *3*, 1201.
15. Burger, A. M.; Dai, F.; Schultes, C. M.; Reszka, A. P.; Moore, M. J.; Double, J. A.; Neidle, S. *Cancer Res.* **2005**, *65*, 1489.
16. (a) Pennarun, G.; Granotier, C.; Gauthier, L. R.; Gomez, D.; Hoffschir, F.; Mandine, E.; Riou, J.-F.; Mergny, J.-L.; Mailliet, P.; Boussin, F. D. *Oncogene* **2005**, *24*, 2917; (b) Gomez, D.; O'Donohue, M.-F.; Wenner, T.; Douarre, C.; Macadré, J.; Koebel, P.; Giraud-Panis, M.-J.; Kaplan, H.; Kolkes, A.; Shin-ya, K.; Riou, J.-F. *Cancer Res.* **2006**, *66*, 6908.
17. Gunaratnam, M.; Riou, J. F.; Neidle, S. et al., to be published.
18. Parkinson, G. N.; Lee, M. P. H.; Neidle, S. *Nature* **2002**, *417*, 876.
19. Burge, S.; Parkinson, G. N.; Hazel, P.; Todd, A. K.; Neidle, S. *Nucleic Acids Res.* **2006**, *34*, 5402.
20. Kan, Z. Y.; Yao, Y.; Wang, P.; Li, X. H.; Hao, Y. H.; Tan, Z. *Angew. Chem. Int. Ed.* **2006**, *45*, 1629.
21. Zhang, N.; Phan, A. T.; Patel, D. J. *J. Am. Chem. Soc.* **2005**, *127*, 17277; Ambrus, A.; Chen, D.; Dai, J.; Bialis, T.; Jones, R. A.; Yang, D. *Nucleic Acids Res.* **2006**, *34*, 2723.
22. Ladame, S.; Schouten, J. A.; Stuart, J.; Roldan, J.; Neidle, S.; Balasubramanian, S. *Org. Biol. Chem.* **2004**, *2*, 2925.
23. Wang, Y.; Patel, D. J. *Structure* **1993**, *1*, 263.
24. Case, D. A.; Cheatham, T. E., III; Darden, T.; Gohlke, H.; Luo, R.; Merz, K. M., Jr.; Onufriev, A.; Simmerling, C.; Wang, B.; Woods, R. *J. Comput. Chem.* **2005**, *26*, 1668.
25. Pettersen, E. F.; Goddard, T. D.; Huang, C. C.; Couch, G. S.; Greenblatt, D. M.; Meng, E. C.; Ferrin, T. E. *J. Comput. Chem.* **2004**, *25*, 1605.
26. Compound **2**: δ_H (400 MHz, $CDCL_3$) 1.85 (br s, 8H), 2.50 (t, 5.6 Hz, 4H), 2.63 (br s, 8H), 2.80 (t, 5.6 Hz, 4H), 4.81 (s, 2H), 7.04 (m, 2H), 7.19 (m, 1H), 7.87–7.89 (m, 6H), 11.50 (s, 2H); *m/z* 602 (MH^+); $C_{34}H_{38}N_6O_2F_2$ requires 601.3097; observed 601.3080. Compound **3**: δ_H (400 MHz, MeOD) 1.86 (s (br), 8H), 2.51 (t, 5.6 Hz, 4H), 2.64 (br s, 8H), 2.81 (t, 5.6 Hz, 4H), 3.68 (s, 6H), 4.80 (s, 2H), 6.34 (m, 1H), 6.46 (m, 2H), 7.07 (m, 2H), 7.82 (m, 2H), 7.91 (d, 9.2 Hz, 2H), 11.52 (s, 2H); *m/z* 625 (MH^+); $C_{36}H_{44}N_6O_4$ requires 625.3497; observed 625.3500. Compound **4**: δ_H (400 MHz, $CDCL_3$) 1.92 (br s, 8H), 2.35 (s, 3H), 2.57 (t, 5.6 Hz, 4H),2,69 (br s, 8H), 2.87 (t, 5.6 Hz, 4H), 4.89 (s, 2H), 7.13–7.20 (m, 3H), 7.24–7.28 (m, 1H), 7.74 (m, 2H), 7.88 (br s, 2H), 7.99 (d, 9.2 Hz, 2H) 11.50 (s, 2H); *m/z* 579 (MH^+); $C_{35}H_{42}N_6O_2$ requires 579.3442; observed 579.3464. Compound **5**: δ_H (400 MHz, $CDCL_3$) 1.94 (s (br), 8H), 2.58 (t, 5.6 Hz, 4H), 2.72 (br s, 8H), 2.88 (t, 5.6 Hz, 4H), 5.03 (s, 2H), 7.43–7.96 (m, 9H), 11.63 (s, 2H); *m/z* 651 (MH^+); $C_{35}H_{38}N_6O_2F_4$ requires 651.3065; observed 651.3049. Compound **6**: δ_H (400 MHz, $CDCL_3$) 1.94 (s, 8H), 2.58 (t, 5.6 Hz, 4H), 2.71 (s, 8H), 2.88 (t, 5.6 Hz, 4H), 5.12 (s, 2H), 7.82–7.99 (m, 9H), 11.65 (s, 2H); *m/z* 701 (MH^+); $C_{36}H_{38}N_6O_2F_6$ requires 701.3033; observed 701.3034. Compound**7**: δ_H (400 MHz, $CDCL_3$) 1.50 (br s, 4H), 1.66 (br s, 8H), 2.52 (br s, 12H), 2.66 (m, 4H), 2.93 (s, 6H), 4.93 (s, 2H), 6.84 (d, J = 8.4 Hz 1H), 7.11 (m, 2H), 7.27 (m, 1H), 7.85 (br s, 2H), 7.88–7.98 (m, 3H), 8.32 (m, 1H), 11.66 (s, 2H); *m/z* 629 (MH^+); $C_{36}H_{42}N_6O_2F_2$ requires 629.3410; observed 629.3429. Compound **8**: δ_H (400 MHz, $CDCL_3$) 1.46 (s (br), 4H), 1.65 (br s, 8H), 2.53 (m, 12H), 2.66 (m, 4H), 3.73 (s, 6H), 4.88 (s, 2H), 5.69 (br s, 1H), 6.40 (br s, 1H), 6.55 (br s, 2H), 7.82–8.06 (m, 6H) 11.65 (s, 2H); *m/z* 654 (MH^+); $C_{38}H_{48}N_6O_4$ requires 653.3810;

observed 653.3821. Compound **9**: δ_H (400 MHz, $CDCL_3$) 1.50 (s (br), 4H), 1.68 (br s, 8H), 2.35 (s, 3H), 2.52 (m, 12H), 2.66 (m, 4H), 4.90 (s, 2H), 5.48 (br s, 1H), 7.18 (m, 4H), 7.83 (br s, 2H), 7.90 (br s, 2H), 7.02 (d, 8.2 Hz, 2H) 11.64 (s, 2H); *m/z* 608(MH^+); $C_{37}H_{46}N_6O_2$ requires 607.3755; observed 607.3786. Compound **10**: δ_H (400 MHz, $CDCL_3$) 1.47 (s (br), 4H), 1.63 (br s, 8H), 2.43 (br s, 12H), 2.58 (m, 4H), 6.67–6.85 (m, 4H), 7.15 (br s, 2H), 7.82 (m, 2H); *m/z* 622 (MH^+); $C_{37}H_{47}N_7O_2$ requires 622.3863; observed 622.3859. Compound **11**: δ_H (400 MHz, $CDCL_3$) 1.52 (br s, 4H), 1.68 (br s, 8H), 2.54 (br s, 12H), 2.66 (m, 4H), 2.93 (s, 6H), 6.72 (d, J = 8.8 Hz 2H), 6.92 (d, J = 8.4 Hz, 2H), 7.23 (m, 2H), 7.94 (m, 4H), 11.63 (s, 2H); *m/z* 623 (MH^+); $C_{37}H_{47}N_7O_2$ requires 622.3864; observed 622.3859.

27. Schultes, C. M.; Guyen, B.; Cuesta, J.; Neidle, S. *Bioorg. Med. Chem. Lett.* **2004**, *14*, 4347.
28. FRET experiments: HPLC purified and desalted oligonucleotide F21T was supplied by Eurogentec. It was annealed at a concentration of 400 nM in buffer (50 mM KCl, 10 mM cacodylic acid, adjusted to pH 7.4 by KOH addition) by heating to 92° for 2 min and allowing to cool to room temperature over 4 h after which it was further diluted to 317 nM with buffer. Stock solutions of ligands were prepared in potassium chloride-cacodylate buffer. 96-well plates (Bio-Rad MLL9651) were prepared with a Gilson Cyberlab C-200 Robotic Workstation, each containing 100 μL aliquots per well with an oligonucleotide concentration of 200 nM and a concentration series between 0.10 and 10.00 μM for each ligand. The wells were read in a DNA Engine Opticon 1 real-time PCR cycler (MJ Research). Fluorescence was measured at 0.5° intervals whilst increasing the temperature from 30° to 100° at a rate of 1°/min. Excitation was at 450–495 nm and detection at 515–545 nm. Data analysis was performed using Origin Pro 7.0 (OriginLab Corporation). Experiments were performed in triplicate and esds are ±0.5°.
29. TRAP assay: the telomerase repeat amplification protocol (TRAP) assay was used to assess the activity of telomerase in the presence of the compounds. It was conducted using a modified version of standard published TRAP protocols.[24] The telomerase enzyme source was a cell extract from exponentially growing A2780 human ovarian carcinoma cells. The TRAP assay was carried out in two steps. First, for the elongation of the primer by telomerase, a TRAP reaction mixture (40 μL) was prepared, containing the TS forward primer (0.1 μg; 5′-AATCCGTCGAGCAGAGTT-3′; Invitrogen, Paisley, UK), TRAP buffer (20 mM Tris–HCl [pH 8.3], 68 mM KCl, 1.5 mM $MgCl_2$ 1 mM EGTA and 0.05% v/v Tween 20), BSA (0.05 μg) and dNTPs (125 μM). Protein (1 μg) was then incubated with the TRAP reaction mixture with or without drug for 10 min at 30°. Subsequently, the telomerase was inactivated by heating to 92° for 4 min and cooling to 10°. During cooling, 10 μL of a PCR mixture containing ACX primer (0.1 μg; 5′-GTG[CCCTTA]$_3$CCCTAA-3′; Invitrogen, Paisley, UK) and *Taq* polymerase (RedHot, AABgene, Surrey, UK) was added to each tube, thus initiating the second step of amplification of the telomerase products. The polymerase chain reaction was carried out in 33 cycles of 92° for 30 s, 55° for 30 s and 72° for 45 s. Finally, the amplified PCR products were run out on a 10% w/v PAGE gel and visualized by staining with SYBR Green I (Sigma). The TRAP products were quantified by fluorescence and the $^{tel}EC_{50}$ values were calculated using GeneTools software (Syngene, Cambridge, UK) and OriginPro 7.0 (Originlab Corp., Northampton, MA). Experiments were performed in triplicate and esds are estimated to be ±0.02 μM. All compounds were examined for their ability to inhibit the activity of TAQ polymerase, and no inhibition was observed at or near the concentrations required for telomerase inhibition. Results from the TRAP assay performed in different laboratories cannot readily be compared since differing experimental protocols are frequently used, and the results presented here should be considered as relative rather than as absolute indicators of telomerase inhibition.